

# Structures of plasma and current in dynamic Z pinches

I. Ya. Butov and Yu. V. Matveev

(Submitted 30 December 1980)

Zh. Eksp. Teor. Fiz. **81**, 560-571 (August 1981)

The dynamics of plasma layers and the structure of the current in a Z-pinch device is experimentally investigated. It is found that the formation of the principal current sheath ends with a disruptive expansion of the sheath, and the pinch breaks up after compression into separate current filaments. It is also shown that the filling of the region outside the pinch with plasma and with currents that alternate in direction is the result of the interaction of current loops (inductors) produced in the magnetic piston after it is compressed by the reflected shock wave. The observed phenomena take place when overheat instability develops and can be realized, e.g., in  $\theta$  pinches, plasma foci, and tokamaks.

PACS numbers: 52.55.Ez, 52.40.Kh

## 1. INTRODUCTION

During the first stage of research into controlled thermonuclear reactions, most experiments were performed with pulsed Z-pinch discharges.<sup>1</sup> Self-compressing discharges, particularly various modifications of the Z pinch, are of practical interest even now. This interest is due to the possibility of obtaining in them a working medium of increased density, so that thermonuclear installations can be decreased in size and the required plasma containment time can be shortened. Other factors are the simplicity of the method of transferring energy to the ions, and the high value of  $\beta$  ( $\beta = 8\pi p/H^2$  is the ratio of the gaskinetic pressure of the plasma to the pressure of the magnetic field), which make the thermonuclear system economical.

Certain experimental results, however, do not make it possible to draw a self-consistent picture of the processes in Z-pinch installations. The reason is the lack of sufficient information on the initial stage of the discharge (gas breakdown, the field skin effect) and on the subsequent dynamics of the high-current plasma. In particular, very few studies were made of the processes

that occur in the time interval between the "singularities" of the discharge current.<sup>1</sup> Thus, e.g., the assumptions that bursts of the pinch to the wall take place after the first singularity, and that the second and succeeding singularities are due to pulsations of the plasma compressed towards the axis, are contradictory and do not agree fully with the observations. The contradictory character of the information makes it difficult to understand the causes of the appearance of nonequilibrium particles. To make more precise the ideas concerning the magnetohydrodynamic phenomena and to find the optimal plasma compression and heating regime, further experimental and theoretical research is necessary.

We present in this paper experimental data on the motion of plasma sheaths in a Z pinch unit in the time interval from the gas breakdown to the second singularity. Certain phenomena (disruptive formation of current sheaths, the multiple onset of current loops in the compressed plasma, the breakup of the expanding plasma into current filaments) have been observed in Z-pinch experiments for the first time ever.

## 2. APPARATUS AND PROCEDURE

The experiments were performed with the "dynamic Z pinch" (DZP, see Fig. 1). The current return lead 2, which encloses a porcelain chamber 3 of diameter 28 cm and length 50 cm, is a solid cylindrical shell. The initial vacuum in the chamber is  $10^{-6}$  Torr; there was no preionization of the working gas ( $H_2$ ,  $D_2$ ), and the initial pressure of the working gas  $p_0 = 3 \times 10^{-1} - 2 \times 10^{-2}$  Torr.

To investigate the dynamics of the glowing plasma sheaths, we used an SFR-2M streak camera.<sup>2</sup> The information on the fine radial structure of the field  $H_r$  (of the current  $I_r$ ) in the central section of the chamber and on the radial structure of the voltage  $V_r$  was obtained using high-frequency magnetic probes and resistive voltage dividers respectively.<sup>3</sup> The plasma jet escaping through the central opening (of 3 mm diameter) in the electrode was registered with diamagnetic  $\sigma - v$  probes by observing the forcing-out of the plasma flux  $\Phi$  by the moving plasma with conductivity  $\sigma$ . The absence of plasma at the chamber wall was confirmed with a compensated probe (one of the probe coils was built into the wall). The discharge current  $I(t)$  was measured with a Rogowski loop.

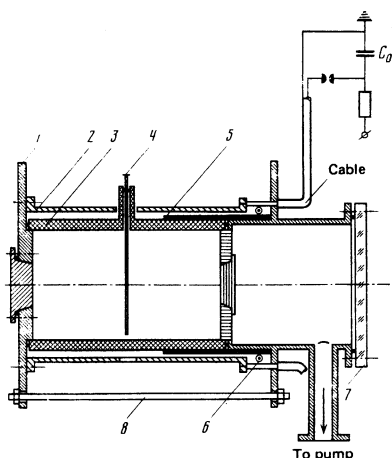


FIG. 1. "Dynamic Z pinch" installation: 1) electrode (copper, aluminum, stainless steel), 2) return current lead, 3) chamber, 4) tube for magnetic probes (quartz), 5) insulation, 6) Rogowski loop, 7) window for photography of the discharges through openings (not shown) in the electrode, 8) tightening screws. The parameters of the setup are: energy in capacitor bank  $W_{C0} = 15$  KJ,  $I_{max} = 3.5 \times 10^5$  A,  $T/2 = 9$   $\mu$ sec.

### 3. INVESTIGATIONS OF THE STRUCTURES OF THE PLASMA (CURRENT) IN A DYNAMIC Z PINCH

**3.1. Gas breakdown and formation of plasma sheaths.** The breakdown of the rarefied gas in the gap between the electrodes was revealed by a glow that was uniform over the chamber diameter (Fig. 2). We denote the vertical boundary of the initial illumination as layer 1 ( $t = 0$ ). Simultaneously with the appearance of layer 1, a brighter plasma sheath ( $\Delta r \approx 5 - 10$  mm) or layer 2 moving away from the wall appears. The luminosity of layer 2 decreases rapidly after moving 3–4 cm away from the wall chamber, and is followed by propagation of a weakly glowing front towards the axis. The velocity  $v_2$  of layer 2 increases with decreasing  $p_0$ . At  $p_0 < 10^{-1}$  Torr we have  $v_2 > 10^7$  cm/sec, and layer 2 reaches the axis before the main plasma sheath, layer 3 (Fig. 2c), is produced at the wall. No expansion of the layer 2 after convergence to the chamber center was observed in the region  $p_0 < 10^{-1}$  Torr.

By the end of the first microsecond from the start of the discharge, the formation of the main plasma sheath—layer 3—is completed. At that time, an abrupt flash of light is produced, located  $\sim 3$  cm away from the wall chamber. At the instant  $t = 1 \mu\text{sec}$ , the current is  $I = 150 - 180$  kA, or  $\sim 70\%$  of the maximum current ahead of the first singularity. The contraction of the layer 3 towards the axis proceeds subsequently either in the form of one brightly glowing sheath (Fig. 2b) or in the form of two (sometimes three) glowing fronts (Fig. 2c). The structure of the layer 3 is determined by the initial gas pressure, by the type of gas, and by the degree to which the chamber has been preconditioned.

At  $p_0 > 2 \times 10^{-1}$  Torr, the layer 3 is preceded, at a distance 2–4 cm, by layer 2. The arrival of layer 2 at the axis is accompanied by the onset of a reflected front. A similar interaction is observed also at  $p_0 \lesssim 2.5 \times 10^{-2}$  Torr, when a pronounced separation of layer 3 into two glowing sheaths takes place. The collision of the reflected front with the second sheath does not affect in

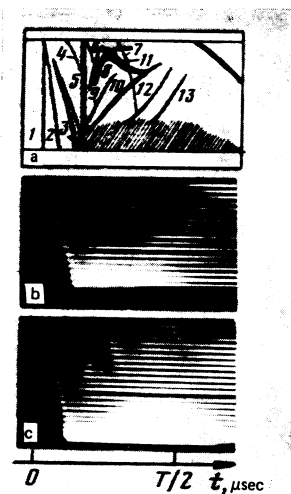


FIG. 2. Streak photographs of discharges in deuterium. Chamber radius 14 cm. a) Synthesized streak photograph (negative), b)  $p_0 = 3 \times 10^{-1}$  Torr, c)  $p_0 = 5 \times 10^{-2}$  Torr.

this case the velocity of the latter towards the axis (Fig. 2a).

At low  $p_0$  ( $< 10^{-1}$  Torr) the layer 3 is followed by the appearance of layers 4, 5, and 6. Layer 4, of thickness  $\leq 1$  cm moves at a distance 6–7 cm from layer 3 with a velocity somewhat larger than that of layer 3. The phase of the maximum energy cumulation in layer 3 is marked by a short-duration ( $\Delta t = 0.2 - 0.4 \mu\text{sec}$ ) and a powerful radiation flash<sup>1,2</sup> (layer 5), which leads to the appearance of layer 6 at the wall of the chamber. The rate of convergence of layer 6 to the axis is close to that of layer 4. Layer 4 is generated at the maximum of the current ahead of the first singularity. Layer 6 is produced in the region of the singularity.

**3.2. Magnetohydrodynamic activity of the pinch after the first compression.** During the lifetime of the plasma formation on the chamber axis ( $\sim 10 \mu\text{sec}$ ), glowing sheaths are emitted from this formation. Their number and depth of penetration in the wall direction are determined by the pressure and type of the working gas. At increased  $p_0 = (1.5 - 3.0) \times 10^{-10}$  Torr, up to six glowing sheaths are observed (Fig. 2b).

The maximum speed of layers 7 and 8 is  $2.5 \times 10^7$  cm/sec. At high  $p_0$  the thin layer 7 ( $\Delta r < 1$  cm) almost always reaches the walls of the chamber. Layer 11 then goes out of this region. Following the emergence of layers 7 and 8 from the equilibrium pinch, ejection of layers 9, 10, 11, and 12 is observed (Fig. 2a). This is how the volume of the chamber outside the pinch is filled with plasma.

Layer 9 reaches up to  $r \leq 10$  cm without hindering the motion of layer 11 to the axis. Layer 10, carrying a large momentum, stops the layer 11 (Fig. 2b) and reverses its motion.

**3.3. Radial structures of the field  $H_\theta$  (of the current  $I_z$ ) in the central section of the chamber.** Prior to the arrival of the main current sheath (layer 3) at the location of the probes, a uniformly distributed current is registered in the chamber, equal to the current flowing prior to the skinning. The diffusion current decreases with increasing  $p_0$  ( $j_\theta \approx 80$  A/cm<sup>2</sup> at  $p_0 = 3 \times 10^{-2}$  Torr). At  $p_0 = 10^{-1} - 10^{-2}$  Torr, a pronounced skinning of the current takes place correspondingly after  $(1 - 5) \times 10^{-7}$  sec.

After the skinning the current does not break away from the chamber wall before the end of the first microsecond. At the instant  $t = 1 \mu\text{sec}$ , the maximum current density is registered in a shell with  $\sim 1 - 2$  cm and located 2–4 cm away from the wall chamber (the distance decreases with increasing  $p_0$ ). The position of the cylindrical shell with  $j_{\text{max}}$  coincides with the region of the light flash observed at the end of the first microsecond of the discharge developed in (Fig. 2).

Without considering the subsequent distributions of  $H_\theta$  and  $j_z$  at different instants of time (they are qualitatively close to those given in Ref. 4), we shall analyze the signals from the magnetic probes (Fig. 3). The advance of the current-carrying plasma to  $r = 3.5$  cm is marked

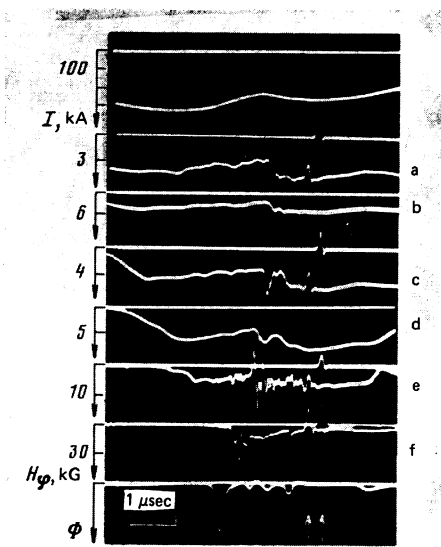


FIG. 3. Dynamics of development of the structures of the field  $H$  (of the discharge current  $I$ ) in the region of the first singularity.  $p_0 = 2 \times 10^{-1}$  Torr  $D_2$ . a)  $r = 13.5$  cm; b)  $r = 11.5$  cm; c)  $r = 9.5$  cm; d)  $r = 7.5$  cm; e)  $r = 5.5$  cm; f)  $r = 1.5$  cm.  $\ast$ ) magnetic flux crowded out in the  $\sigma$ - $\nu$  probe by the plasma jets. The arrows indicate the synchronizing pulses.

by an almost monotonic increase of the signals. In the region  $r < 3.5$  cm, a considerable change takes place in the structure of the field in the current sheath. The field  $H_\phi$  arrives at  $r = \pm 1.5$  cm in the form of a "pedestal" of duration  $0.4 \mu\text{sec}$ , preceding a steeply rising pulse ( $\tau_{r,r} < 50$  nsec). In the region of high  $p_0$ , the current connected with the field pulse sometimes exceeds by 1.5–2 times the current in the discharge circuit. The strong field  $H_\phi$  localized inside the magnetic piston is registered at  $r = 1.5$  cm ahead of the first singularity (Fig. 4, curve a).

To study the processes contributing to the appearance of current loops in the plasma, a diamagnetic probe was used (see Sec. 3.5). At high  $p_0$ , an ionized-gas pressure pulse is registered on the chamber axis (Fig. 3). The interaction of the reflected shock wave with the magnetic field profile moving towards the axis contributes to localization of  $H_\phi$  in narrow zones ( $\Delta r < 1$  cm) within the current layer. The delay in the registration of the  $H_\phi$  pulses, which increases with the radius (Fig. 3), points to a rapid advance of one to three closed current loops to the wall. The time from the instant of the

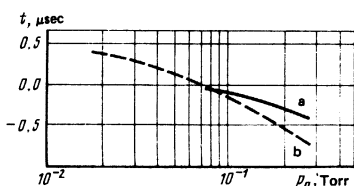


FIG. 4. Instants of appearance of steeply growing pulse of  $H_\phi$  at  $r = 1.5$  cm (a) and of the maximum signal from the diamagnetic probe (b) relative to the instant of the first singularity ( $t_1 = 0$ ).

first singularity to the maximum pressure pulse is shown in Fig. 4 (curve b).

The velocity of the first current loop ejected from the pinch is  $(2-4) \times 10^7$  cm/sec and equals the velocity of the layer 7. Layer 8 moves towards the wall at about the same velocity. A small decrease of the velocity of layer 8 is noted only starting with  $r = 9.5$  cm, i.e., after the layers 7 and 8 are visualized (interaction with the gas remaining at the wall and with layer 6). Proximity of the field discontinuities to the light fronts is noted also subsequently. Thus, e.g., at  $0.6-0.7 \mu\text{sec}$  after the instant  $t_1$ , a field discontinuity  $H_\phi = 3.5$  kG is registered at  $r = 5.5$  cm and moves up to  $r = 9.5$  cm with an average velocity  $4 \times 10^6$  cm/sec. At the same time and with the same velocity, layer 9 moves towards the wall and vanishes at  $r = 9-10$  cm. The evaporation of the probe tube makes it difficult to relate the light fronts to the  $H_\phi$  pulses at later instants of time.

Ejection of current loops that are symmetrical with respect to the chamber axis is observed in the entire range of  $p_0$ . On going to low  $p_0$  this process becomes less pronounced. Addition of 30% nitrogen to the deuterium at  $p_0 = 1.8 \times 10^{-2}$  Torr leads to formation of only one loop in the pinch.

At  $p_0 \geq 10^{-1}$  Torr, half the total current flows in the dark region with  $\Delta r = 1-1.5$  cm adjacent to the outer boundary of layer 3. The remaining current flows predominantly in layer 3. On going to smaller  $p_0$  ( $< 10^{-1}$  Torr) the diffuse current through the cross section bounded by layer 3, together with the current in the region between the glowing sheaths of layer 3, amounts to 30% of the total current. Approximately 50% of the current is concentrated in the region of the second sheath.

3.4. Azimuthal structures of the field  $H_\phi$  (of the current  $I_z$ ) in the central section of the chamber. During the course of filling the region outside the pinch with plasma and with current, a sudden reversal of the sign of the magnetic field of the current is observed (Fig. 5). This reversal starts predominantly near the axis and propagates further towards the chamber wall. The behavior of this phenomenon is illustrated in Fig. 6.

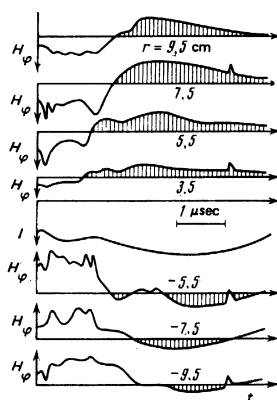


FIG. 5. Reversal of the sign of the field  $H_\phi(r, t)$  in the first half-cycle of the current flow.  $p_0 = 2 \times 10^{-2}$  Torr  $D_2$ .

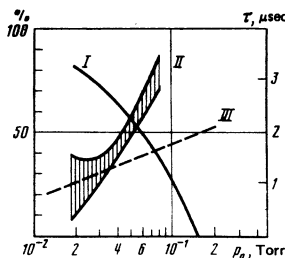


FIG. 6. Probability of filament formation (I) in the first half-cycle of the current, time (II) from the first singularity of the current to the start of the filament formation and the interval between the first and second singularities (III). The neutrons are registered at  $p_0 \leq 2.5 \times 10^{-2}$  Torr  $D_2$ .

It has been established that the reversal of the field is a property of discharges in thoroughly preconditioned chambers with an initial vacuum  $< 10^{-5}$  Torr. Addition of heavy gas to the deuterium (e.g., 0.3–0.5% Ar) decreases considerably the probability of decay of the pinch and of the plasma sheaths into current filaments. A similar influence of additives on the generation of hard radiation was noted earlier.<sup>1</sup>

**3.5. Maximum compression of the plasma and singularities.** The use of  $\sigma-v$  probes has made it possible to obtain more complete information on the dynamics of Z pinches in the region near the axis (Fig. 3; Sec. 3.3). It was observed that the time at which the plasma reaches the chamber axis does not coincide in practice with the instant of the first singularity (Fig. 4). The plasma pulsations noted after the singularity do not leave any markers on the discharge current. With decreasing  $p_0$ , the pulsation frequency increases ( $f = 4-10$  MHz). The time interval during which the plasma flows out is then increased to  $2 \mu\text{sec}$  and the pressure at the axis does not increase at the instant of the second singularity. Magnetic probes frequently likewise fail to indicate contraction of the current in the region with  $r = \pm 1.5$  cm at that time, whereas the second singularities appears regularly on the discharge-current oscillograms at  $p_0 < 10^{-1}$  Torr.

Phasing of the light fronts with the  $\sigma-v$  probe signals has shown that at low  $p_0$  the low-amplitude pressure pulse ahead of the singularity correlates with the arrival of the first luminous sheath of layer 3 at the axis (Fig. 2). The maximum signal from the probe corresponds to the arrival of the second luminous sheath. Since the region of the maximum pressure is localized in the region of the outer boundary of layer 3, it becomes clear why there is no disturbance of the dynamics of this sheath when it collides at the instant of current singularity with the first sheath that expands away from the axis. Similar comparisons made at high  $p_0$  ( $> 10^{-1}$  Torr) point to a correlation between the pressure pulse that precedes the first singularity and the layer 2 arriving at the axis.

The use of a second  $\sigma-v$  probe has made it possible to determine the rate of axial outflow of the plasma. With decreasing  $p_0$ , the plasma axial velocity increases to  $10^7$  cm/sec. Taking into account the proximity of this

value to the compression velocity, this is evidence of heating of the deuterons to  $\sim 100$  eV.

We thus conclude that (1) the plasma frequently does not arrive at the axis at the instant of the first singularity, and 2) the second and succeeding current singularities are not connected as a rule with radial oscillations of the pinch, as was assumed earlier.<sup>1</sup>

**3.6. Radial distributions of the voltage in the gap between the electrodes.** The information obtained with the voltage dividers<sup>3</sup> pertains to the case when there is no plasma breakup into current filaments. Measurements of  $V_z(r, t)$  confirm the presence of a current structure in the plasma sheath. When the plasma expands one observes, e.g., a change in the polarity in the internal regions of the chamber. A pulse of reverse polarity (a backward current) is carried towards the chamber wall with velocity  $\sim 10^7$  cm/sec.

On going to lower  $p_0$ , the negative  $V_z$  bursts vanish first at the chamber wall (the streak photographs do not show the arrival of layer 9 in these regions when  $p_0$  is decreased). This is followed by the vanishing of the bursts at  $r = 2$  cm, and at  $p_0 = 2 \times 10^{-2}$  Torr a reverse voltage is registered only at  $r = 4$  cm.

**3.7. Plasma in the region next to the wall.** The dragging of the plasma towards the axis and its appearance at the chamber wall were investigated with the aid of a compensated probe (Fig. 7). Good correlation was observed between the  $\Delta H_\phi$  signals and the phenomena noted when the discharges were photographed. Thus, the stage of formation of the current sheath (prior to its detachment from the wall) has a duration  $\sim 1 \mu\text{sec}$ . The pulses that appear later correspond to the luminous layers 4, 6, 7, 8, and 11.<sup>1</sup> During the time that layers 7 and 8 hit the wall, reversal of the sign of  $\Delta H_\phi$  is observed, indicating that the field  $H_\phi$  at the wall exceeds the vacuum value. In earlier experiments<sup>5</sup> a pressure up to 1–2 atm on the wall was observed at that instant.

The reversal of the sign of  $\Delta H_\phi$  is observed also during the stage of formation of the layer 3 (Fig. 7b). If there is no breakup of the plasma layer 3 into current filaments, this indicates that a fast front that clamps the magnetic field to the wall moves from the region of the flash of layer 3.

Effective screening (which stops the breakup) of the pinch of the plasma at the wall is noted at  $p_0 < 10^{-1}$  Torr

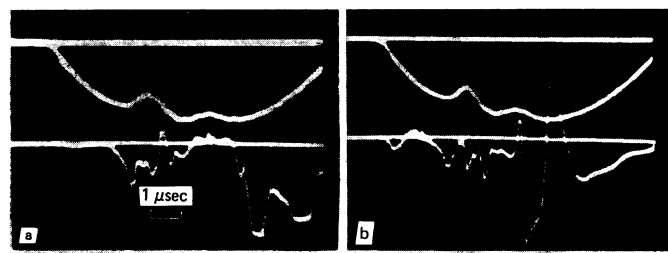


FIG. 7. Compensated-probe signals phased-in with the current  $I$  (upper curves): a)  $p_0 = 7 \times 10^{-2}$  Torr  $D_2$ , b)  $p_0 = 5 \times 10^{-2}$  Torr  $D_2$ .

after the second singularity. On going to higher  $p_0$ , the signal from the compensated probe, which is of considerable amplitude and duration, shifts towards the end of the current half-cycle.

#### 4. DISCUSSION OF RESULTS

We investigated in the Z-pinch experiments effects that were not noted earlier and develop in the time interval from the gas breakdown to the second singularity of the discharge current. The most interesting among them are the following:

- a) The presence of fast luminous fronts preceding the shock wave.
- b) The motion of the plasma towards the wall after the formation of the principal plasma sheath is completed.
- c) A difference between the instants of the singularities and the instants of the maximum compression of the plasma on the chamber axis.
- d) Formation of a number of close current loop in the interior of the pinch and their ejection to the periphery.
- e) Breakup of the plasma in the region of the second singularity into current filaments.

We shall discuss these effects in the same sequence as above.

The motion of the fast front ( $v_{\max} \approx 3 \times 10^7$  cm/sec) and the displacement of the plasma towards the wall are known from experiments on plasma acceleration.<sup>6</sup> There is at present, however, no unambiguous treatment of these phenomena. From the experimental data presented in Sec. 3 it follows that the skinning of the field in the discharge chamber does not prevent flow of current in the interior sections of the chamber. Therefore the motion of the ionized medium towards the axis may be due to an electromagnetic force distributed over the volume. The estimated values of the density of the charged particles in the fast front, calculated at a distance  $r=10$  cm from the Alfvén velocity, amount to  $\sim 7 \times 10^{12}$  cm<sup>-3</sup> and are close to those registered in accelerators.<sup>7</sup>

At low  $p_0$ , the ion mean free path is commensurate with the chamber radius. Thus, at  $p_0 = 3 \times 10^{-2}$  Torr the path of the deuteron up to nonresonant charge exchange is  $\sim 5$  cm. Taking this circumstance into account, as well as the decrease of the diffuse current with increasing  $p_0$ , the absence of a fast front in the region  $p_0 \geq 10^{-1}$  Torr becomes understandable. The motion of the ionized medium is limited under these conditions by the growing interaction of the medium with the neutral gas.

The motion of the fast front to the axis takes place simultaneously with the skinning of the current and with the radial displacement of the charged particles. As a result, the maximum current density is registered by the instant  $t=1$   $\mu$ sec in the region  $\Delta r=1-2$  cm located 2-4 cm away from the wall. The appearance of a brightly glowing sheath (layer 3) in the region of increased current density should be attributed to the production of a high-temperature T-layer<sup>8</sup> (the nonlinear stage of the superheat instability<sup>9</sup>). The disruptive expansion of the

T-layer plasma is registered by the compensated probe and is marked by a flash of light from the excited atoms. An example illustrating the burst of two fronts in the course of expansion of the T layer is Fig. 8, which shows a photograph of a  $\theta$  pinch in helium.

In the experiments performed, the arrival of the ionized medium at the chamber axis was registered at high  $p_0$  prior to the first singularity. In the region of low  $p_0$ , the plasma contraction is completed after the singularity. In both cases, the appearance of a dense plasma at the axis is not accompanied by a maximum contraction of the current. The experimental data at low  $p_0$  (two and more singularities) can be explained by assuming a connection between the second and the subsequent rarely occurring singularities with a drift of the plasma sheaths towards the axis (layers 6 and 11). Numerical experiments<sup>2</sup> confirm this, if the mass of the sheaths is close to the mass of the pinch. The compression of layer 6 towards the wall by layers 7 and 8 at high  $p_0$  leads to formation of a heavy sheath, whose slower displacement does not cause appearance of a second singularity.

It follows from the experiment that the first singularity corresponds to the phase of maximum energy cumulation. In the region of high  $p_0$  ( $>10^{-1}$  Torr) this cumulation sets in when the reflected shock wave interacts with the current sheath several centimeters away from the axis. The rapid compression of the current-carrying plasma by the reflected wave disrupts the diffusion profile of the magnetic field distributed in the plasma. The result is formation of a comb-like field structure similar to that obtained in the calculations of Ref. 10, i.e., closed current loops<sup>2</sup> (inductons) appear. The interaction of the inducton leads to ejection of one or several of them towards the chamber wall. This is how the region outside the pinch is rapidly ( $\Delta t < 1$   $\mu$ sec) filled with plasma.

The current loops inside the pinch at small  $p_0$  are the result of the initial radial inhomogeneity of the current distribution and of the plasma density. However, the formation of current structures in a relatively homogeneous and dense plasma seems to indicate a multiplication<sup>8</sup> of the perturbation of  $H_\theta$  initially produced on its inner boundary (the freezing-in of the field).

The experimental results, which point to excitation of inductons, explain the previously observed multiple

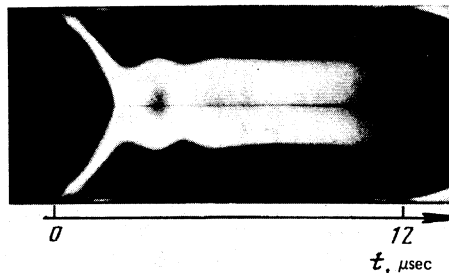


FIG. 8. Streak photograph of  $\theta$  pinch in helium, illustrating the jets from two fronts in the phase of formation of the current sheath ( $p_0 = 10^{-1}$  Torr).

changes of the direction of the current  $I_z$  along the radius of the chamber,<sup>4</sup> the considerable growth of the pressure at its wall,<sup>5</sup> and others. Similar phenomena are apparently responsible for the rapid expansion of the plasma<sup>11</sup> and its ejection from the region of interaction of the axial shock waves (the region of "breaks" in the pinches), observed in Z-pinch devices.<sup>12,13</sup> Similar structures were noted also in  $\theta$  pinches.<sup>2</sup>

We discuss further the breakup of the pinch plasma into separate current filaments (Sec. 3.4). It develops mainly after the first singularity. The breakup probability increases with decreasing  $p_0$  and with decreasing plasma conductivity. Addition of an impurity eliminates the filament formation. A qualitative analysis points to the possibility of explaining the filament formation from the point of view of overheating instability.<sup>14</sup> The low conductivity of the medium surrounding the section with increased current density ensures electromagnetic separation of these regions.

The breakup of plasma into structures is attracting ever increasing attention. The reason is that such states are realizable in a large number of thermonuclear installations (e.g., in tokamaks<sup>15</sup>) and the possibility of explaining the acceleration of the charged particles.<sup>16</sup>

## CONCLUSION

On the basis of the investigations performed, we have obtained the following results.

1) We have shown that the breakdown of the gas ( $H_2$ ,  $D_2$ ) and the formation of the current sheath are accompanied by two phenomena hitherto not observed in Z-pinch devices. Breakdown of a rarefied gas produces a rapid leading layer; the formation of the current sheath at the chamber wall culminates in a disruptive expansion of the plasma.

2) We have found that contraction of the current sheath at  $p_0 > 10^{-1}$  Torr takes place in accordance with the premises of the "magnetic piston plus shock wave" model. At  $p_0 < 10^{-1}$  Torr the more acceptable is the "snowplow" model. The results determine the correctness of the choice of model in the theoretical investigation of such self-contracting discharges.

3) A connection is established between the second and succeeding singularities, observed in the discharge current, on the one hand, and the drift motion of the light plasma sheaths towards the axis (shunting breakdowns) on the other.

4) Information was obtained on a new form of magnetohydrodynamic activity of a high-current plasma. This form of activity, which does not upset the equilibrium of the pinch, manifests itself in a coaxial stratification of the Z pinch and in an ejection of surface sheaths. Filling of the region outside of the core of the pinch with plasma and with currents that change direction takes place as a result of the interaction of several current loops produced in the magnetic piston as it is compressed by the reflected shock wave. The current registered in the

loops is 1.5–2 times larger than the current in the power-supply circuit.

5) Breakup of hydrogen plasma expanding after the instant of the first singularity into separate current filaments was observed. The character of the qualitative dependences of the phenomenon on  $j$ ,  $\sigma$ , and  $p_0$  indicates that it is due to overheating instability.

The results point to the need of an experimental study of the regimes of optimal contraction of the plasma (for example, optimal contraction<sup>2,17</sup> of multiple-sheath plasma formations<sup>18</sup>). Also worthy of serious attention is the protection of the wall (by a gas "jacket" etc.). This problem has not received so far due attention in investigations of plasma with high values of  $\beta$  and with short Lawson containment times. In our experiments the energy radiated from the plasma during the  $3 \times 10^{-7}$  sec of the maximum contraction phase is sufficient to heat the inner surface of the chamber to the melting temperature. For example, 0.12 J/cm<sup>2</sup> is necessary to heat the surface of a quartz chamber to the melting point. Numerical simulation of the influence of impurities on the radiative properties of a Z pinch, performed under the conditions of the dynamic Z pinch (DZP) setup,<sup>19</sup> has indicated the possibility of the release of a large amount of energy during that time (~2.5 kJ or ~0.8 J/cm<sup>2</sup>). The observed magnetohydrodynamic activity of self-contracting discharges also contributes to evaporation of the wall.

We take pleasure in thanking corresponding member of the Georgian Academy of Sciences R. G. Salukvadze for supporting the work and for interest, S. P. Kurdyumov, Yu. P. Popov, and T. I. Filippov for numerous discussions of the results, and V. I. Baryshev and L. P. Stupnitskaya for help with the experiments.

<sup>1</sup>The rapid departure of layers 4 and 6 indicates that their mass is low.<sup>2</sup>

<sup>1</sup>L. A. Artsimovich, *Upravlyaemye termoyadernye reaktsii* (Controlled Thermonuclear Reactions), Fizmatgiz, 1961, Chap. 5.

<sup>2</sup>I. F. Kvartskhava, Yu. V. Matveev, I. Ya. Butov, A. A. Samarskiy, S. P. Kurdyumov, and Yu. P. Popov, 5th Int. Conf. on Plasma Phys. and Contr. Nucl. Fus. Res. (Tokyo 1974), IAEA, Vienna, 1975, Vol. 3, p. 149.

<sup>3</sup>I. F. Kvartskhava, Yu. V. Matveev, and N. G. Reshetnyak, *Pis'ma Zh. Eksp. Teor. Fiz.* 15, 619 (1972) [*JETP Lett.* 15, 437 (1972)].

<sup>4</sup>V. S. Komel'kov, Yu. V. Skvortsov, and S. S. Perevitinov, Proc. 2nd Internat. Conf. on Peaceful Uses of Atom. Energ., Geneva, 1958, Papers by Soviet Scientists [in Russian], Atomizdat, 1959, p. 53.

<sup>5</sup>N. V. Filippov, in: *Fizika plazmy i problema upravlyaemykh termoyadernykh reaktsii* (Plasma Physics and the Problem of Controlled Thermonuclear Reactions), Vol. 2, AN SSSR, 1958, p. 231.

<sup>6</sup>I. M. Zolototrubov, V. A. Kiselev, and Yu. M. Novikov, in: *Issledvaniya plazmennykh sgustkov* (Plasmon Research), Kiev, Naukova dumka, 1965, p. 148.

<sup>7</sup>A. A. Kamykov, S. A. Trubchaninov, V. A. Naboka, and L. A. Zlatopol'skiy, in: *Fizika plazmy i problemy UTS* (Physics of Plasma and of Controlled Thermonuclear Fusion), Kiev, Naukova dumka, Vol. 4, 1965, p. 256.

- <sup>8</sup>A. A. Samarskiĭ, S. P. Kurdyumov, Yu. N. Kulikov, L. V. Leskov, Yu. P. Popov, V. V. Savichev, and S. S. Filippov, Dokl. AN SSSR 206, 307 (1972) [Sov. Phys. Dokl. 17, 871 (1973)].
- <sup>9</sup>B. B. Kadomtsev, in: Voprosy teorii plazmy (Problems of Plasma Theory), Atomizdat, 1963, Vol. 2, p. 132.
- <sup>10</sup>N. V. Dmitrenko and S. P. Kurdyumov, Self-Similar Compression of a Finite Plasma Mass in Z- and  $\theta$ -Pinch Problems, Preprint Inst. Appl. Mech. USSR Academy of Sciences, No. 19, 1974; Prikl. Mat. Tekh. Fiz. No. 1, 3 (1977).
- <sup>11</sup>P. D. Morgan, N. T. Peacock, P. Cloth, *et al.*, 6th Europ. Conf. on Contr. Fusion and Plasma Phys. (Moscow 1973), Vol. 1, 1973, p. 359.
- <sup>12</sup>A. Folkierski, P. G. Frayne, and R. Latham, Int. Conf. on Plasma Phys. and Contr. Nucl. Fusion Res. (Salzburg, 1961). Nucl. Fus. Suppl., Pt. 2, 1962, p. 627.
- <sup>13</sup>V. A. Gribkov, V. M. Korzhavin, O. N. Krokhin, G. V. Sklizkov, I. V. Filippov, and T. I. Filippova, Pis'ma Zh. Eksp. Teor. Fiz. 15, 329 (1972) [JETP Lett. 15, 232 (1972)].
- <sup>14</sup>V. S. Sokolov, Izv. SO AN SSSR ser. Tekhn. Nauk 13, No. 3, 86 (1973).
- <sup>15</sup>B. B. Kadomtsev, Fizika plazmy 1, 710 (1975) [Sov. J. Plasma Phys. 1, 389 (1975)].
- <sup>16</sup>S. I. Syrovatskiĭ, Astron. Zh. 43, 340 (1966) [Sov. Astron. 10, 270 (1966)].
- <sup>17</sup>S. K. Zhdanov and V. A. Trubnikov, Pis'ma Zh. Eksp. Teor. Fiz. 21, 371 (1975) [JETP Lett. 21, 169 (1975)].
- <sup>18</sup>Yu. V. Matveev and I. F. Kvartskhava, 8th Europ. Conf. on Contr. Fusion and Plasma Phys. (Prague, 1977), Vol. 1, 1977, p. 87.
- <sup>19</sup>G. V. Danilova, S. P. Kurdyumov, Yu. P. Popov, A. A. Samarskiĭ, and L. S. Tsareva, Calculation of High-Current Discharges with Allowance for Secondary-Breakdown Effects, [in Russian], Preprint No. 6, Inst. Appl. Mech. USSR Acad. Sci., 1974.

Translated by J. G. Adashko